Similarities and Differences between Organic Cation Inhibition of the Na,K-ATPase and PMCA†

Craig Gatto,‡ Jeff B. Helms,‡ Megan C. Prasse,‡ Sheng-You Huang,§ Xiaoqin Zou,§ Krista L. Arnett,§,|| and Mark A. Milanick*,||

Division of Biomedical Sciences, Department of Biological Sciences, Illinois State University, Normal, Illinois 61790-4120, Dalton Cardiovascular Research Center & Department of Biochemistry, University of Missouri, Columbia, Missouri 65211, Department of Medical Pharmacology and Physiology, School of Medicine, and Dalton Cardiovascular Research Center, University of Missouri, Columbia, Missouri 65211

Received April 5, 2006; Revised Manuscript Received August 25, 2006

ABSTRACT: The effects of three classes of organic cations on the inhibition of the plasma membrane Ca pump (PMCA) were determined and compared to inhibition of the Na pump. Quaternary amines (tetramethylammonium, tetraethylammonium, and tetrapropylammonium, TMA, TEA, and TPA, respectively) did not inhibit PMCA. This is *not* to imply that PMCA is inherently selective against monovalent cations because guanidine and tetramethylguanidine inhibited PMCA by competing with Ca^{2+}. The divalent organic cation, ethyl diamine, inhibited PMCA but was not competitive with Ca^{2+}. In contrast, propyl diamine did compete with Ca^{2+} and was about 10-fold more potent than butyl diamine in inhibiting PMCA. For the Na pump, both TEA and TPA inhibited, but TMA did not. TEA, guanidine, and tetramethylguanidine inhibition was competitive with Na^+ for ATPase activation and with K^+ for pNPPase activation, both of which are cytoplasmic substrate cation effects. Thus, these findings are consistent with TEA, guanidine, and tetramethylguanidine inhibiting from the cytoplasmic side of the Na pump; in contrast, we have previously shown that TPA did not inhibit from the cytoplasmic side. The divalent alkane diamines ethyl, propyl, and butyl diamine all inhibited the Na pump and all competed at the intracellular surface. The order of potency was ED > PD > BD consistent with an optimal size for binding; similarly, for the quaternary amines TMA is apparently too small to make appropriate contacts, and TPA is too large. Homology models based upon the high-resolution SERCA structure are included to contextualize the kinetic observations.

Active transport systems couple the energy of ATP hydrolysis to the movement of molecules. P-type ATPases are a subclass of active transporters that contain a covalent phosphointermediate in their transport cycle. One subclass of P-type ATPases is the P_2-type family, which transports alkali metals and includes members such as the H,K-ATPase, the Na,K-ATPase, the plasma membrane calcium pump (PMCA),[1] and the sarcoplasmic reticulum Ca pump (SERCA) (for review see refs *1* and *2*). These transporters obviously play a crucial role in many cellular functions. An understanding of the mechanism that converts the chemical energy stored in ATP to the mechanical energy required for the movement of molecules remains a key goal of many membrane transport studies. Functionally, all the P_2-type pumps are modeled with a similar kinetic cycle based upon the Albers-Post model (Figure 1) (*3*, *4*). This kinetic cycle can be divided into two half cycles: for the Na pump, the efflux half cycle including the binding of cytoplasmic 3-Na^+, Mg^{2+} and ATP, the catalytic autophosphorylation of the pump, occlusion and subsequent release of 3-Na^+ extracellularly and ADP intracellularly. The influx half cycle involves binding of extracellular 2-K^+ to the phosphorylated pump, followed by dephosphorylation, release of Pi, and occlusion and subsequent release of 2K^+ intracellularly. For PMCA, 1-Ca^{2+} replaces 3-Na^+ and H^+ replaces 2-K^+; the Ca/H stoichiometry for PMCA remains unsettled (see, e.g., refs *5* and *6*). In addition to hydrolyzing ATP, the Na pump also hydrolyzes pNPP. While high ATPase activity requires both Na^+ and K^+, only K^+ is required for pNPPase activity. Drapeau and Blostein (*7*) showed that cytoplasmic K^+ was

† This work was supported by the following grants (listed alphabetically): American Heart Association 030161N (C.G.), AHA 0265293Z (X.Z.), AHA Predoctoral Fellowship 0315236Z (J.B.H.), National Institutes of Health DK37512 (M.A.M.), NIH, DK61529 (X.Z.) and NIH GM 061583 and NSF MCB-0347202 (C.G.). Software support from the Tripos, Inc. (St. Louis, MO) to X.Z. is also gratefully acknowledged.

* To whom correspondence should be addressed: Mark A. Milanick, Ph.D., Dalton Cardiovascular Research Center, 134 Research Park Drive, University of Missouri, Columbia, MO 65211. Phone: (573) 882-8055. FAX: 573-884-4232. E-mail: milanickm@missouri.edu.

‡ Illinois State University.

§ Dalton Cardiovascular Research Center & Department of Biochemistry, University of Missouri.

|| Department of Medical Pharmacology and Physiology, School of Medicine, and Dalton Cardiovascular Research Center, University of Missouri.

[1] Abbreviations: PMCA, plasma membrane Ca-ATPase; SERCA, sarco/endoplasmic reticulum Ca-ATPase; GUA, guanidine; TMG, tetramethylguanidine; TMA, tetramethylammonium; TEA, tetraethylammonium; TPA, tetrapropylammonium; ED, ethyl diamine; PD, propyl diamine; BD, butyl diamine; pNPP, *para*-nitrophenyl phosphate; NMDG, *N*-methyl-D-glucamine.

10.1021/bi060667j CCC: $33.50
Published on Web 10/13/2006

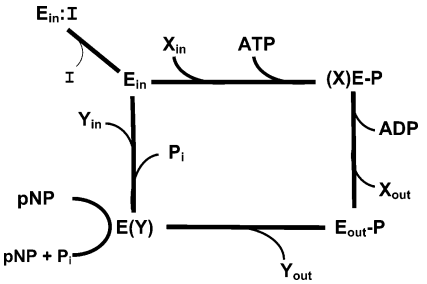

FIGURE 1: A simplified kinetic scheme of a general P-type ATPase cycle. The upper left corner conformation, E_{in}, has the cation site open to the cytoplasm. In this conformation, the cytoplasmic cation X binds to the enzyme along with ATP to produce the phosphorylated intermediate (E_{in}-P). For the Na pump, X_{in} is Na^+; for PMCA X_{in} is Ca^{2+}. An ensuing conformational change opens the cation site to the extracellular space and releases the bound cation to the outside (X_{out}). The pump can now bind Y_{out} and the extracellular access gate is closed prompting the hydrolysis of the phosphointermediate. For the Na pump, Y_{out} is K^+; for PMCA Y_{out} is H^+. A conformational change opens the cation site to the inside and releases the bound cation (Y_{in}). Although the exact Na pump conformation that mediates pNPPase activity is uncertain, it is clear that K^+ binding from the cytoplasm is necessary for the reaction. For simplicity, we have associated the pNPPase activity to the K-occluded form of the enzyme (compare Post et al., 1972), but we are open to alternative possibilities. An inhibitor (I) binding to the cytoplasmic cation site is depicted as a dead-end inhibitor to E_{in}.

sufficient to activate the pNPPase activity. When Na^+_{cyt} was present, extracellular K^+ had a modulatory role. Consequently, pNPPase activity is an efficient assay to examine K^+ binding to the cytoplasmic site in the Na pump when Na is absent.

Organic cations have proved particularly valuable in studies of Na^+ and K^+ transport. Guanidine ions tend to bind better to Na^+ sites; for example, amiloride derivatives inhibit ENaC and Na/H exchange. Quaternary amines tend to bind better to K^+ sites. Despite several studies of organic cation inhibition on the Na pump, only a few studies have examined organic cation inhibition of PMCA. The calcium channel blockers, verapamil, diltiazem, and bepridil (*8*), as well as ruthenium red and compound 48/80 inhibit PMCA (*9*). In all cases, V_{max} was reduced, implying that they did not compete with calcium.

High-resolution crystal structures of several enzyme conformations of SERCA have made key contributions to our understanding of P_2-type pumps (*10*−*17*). Crystal structures of the two major cation bound intermediates, calcium bound and presumably proton bound, have been obtained. The latter required the presence of thapsigargin. More recently, several structures related to a variety of the phosphointermediate states have been obtained (*15*−*17*). However, as yet, there is not a crystal structure for SERCA in which the transport site is empty and open to the cytoplasm.

In the crystal structure of SERCA, Glu^{309} appears to control access to the transport sites in the membrane (*18*). Just to the cytoplasmic side of Glu^{309} is a pocket with several anionic side chains that have been proposed to serve as an access region that the cations must pass through on their way to the transport site (*19*). Schneeberger and Apell (*19*) have provided evidence that a number of organic cations can bind to a kinetically defined access region but are not able to be occluded.

Guanidines	Quaternary Amines	Diamines
		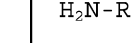

Guanidines		Quaternary Amines		Diamines	
Cation	R =	Cation	R =	Cation	R =
GUA	H	TMA	CH_3	ED	CH_2CH_2
TMG	CH_3	TEA	CH_3CH_2	PD	$CH_2CH_2CH_2$
		TPA	$CH_3CH_2CH_2$	BD	$CH_2CH_2CH_2$ CH_2

FIGURE 2: Chemical structures of organic cations. The eight different organic cations used for this study are shown. The R-groups represent the defined alkyl groups at the respective positions of the three distinct amine containing compounds. Abbreviations: GUA, guanidine; TMG, tetramethylguanidine; TMA, tetramethylammonium; TEA, tetraethylammonium; TPA, tetrapropylammonium; ED, ethyl diamine; PD, propyl diamine; and BD, butyl diamine.

In this study, we compared Na,K pump and PMCA inhibition by organic cations. Organic cations that differed in size, shape, charge, and charge distribution were chosen to gain a better understanding of the properties of cation binding and selectivity of these two pumps. The monovalent cation quaternary amines (tetramethylammonium, tetraethylammonium, and tetrapropylammonium, TMA, TEA, TPA, respectively) are unable to form hydrogen bonds, and the positive charge (on nitrogen) is localized at the center of the compound sterically hindered from direct contact with amino acid side chains. The guanidines (guanidine and tetramethylguanidine, GUA and TMG, respectively) are able to form hydrogen bonds and have the positively charged nitrogen located at the surface of the ligand and therefore could have stronger electrostatic interactions with the negatively charged residues of the pumps. The alkane diamines (ethyl, propyl, and butyl diamine, ED, PD, and BD, respectively), unlike quaternary amines, have two separate localized positive charges that retain the ability to form hydrogen bonds. The various organic cations used in this study are shown in Figure 2. Preliminary results of this work have been presented to the Biophysical Society (*20*) and the Society of General Physiologists (*21*).

EXPERIMENTAL PROCEDURES

Materials. γ[^{32}P]ATP was from Perkin-Elmer Life Sciences. Hydrochloric acid, sodium phosphate, potassium chloride, sodium chloride, sucrose, EDTA, Folin's reagent, imidazole, magnesium chloride, Na_2ATP, sodium bicarbonate, sodium chloride, antipain, pepstatin, leupeptin, phenylmethanesulfonyl fluoride, HEPES, and Trizma base were from Sigma (St. Louis, MO); tetramethylammonium, tetraethylammonium, tetrapropylammonium, guanidine, tetramethylguanidine, ethyl diamine, propyl diamine, and butyl diamine were from Fisher (Fairlawn, NJ). Dog kidneys were salvaged from euthanized dogs that were part of approved IACUC experiments and were the kind gift of Dr. James L. Cook (University of Missouri-Columbia).

Na,K-ATPase Purification from Dog Kidney. Na,K-ATPase was purified from dog kidney as described by Jorgensen (*22*). Briefly, the outer medulla was dissected from five dog kidneys and then homogenized in a blender in a

medium containing 250 mM sucrose, 25 mM imidazole, and 1 mM EDTA (pH = 7.2). The homogenate was filtered through four layers of cheesecloth, and the filtrate was centrifuged at 10000*g*, 15 min. The supernatant liquid was collected and once again centrifuged at 10000*g*, 15 min. These low-speed centrifugation steps remove a significant portion of cellular debris from the microsomal fractions. The supernatant liquid was collected from the second spin, and the microsomal fraction was sedimented at 65000*g*, 1 h. The pellets were collected and resuspended in the above homogenizing medium with the addition of 3 mM ATP to a protein concentration of 6 mg/mL. The microsomal preparation was incubated with ATP present for 10 min and then diluted to a final concentration of 2 mg/mL with 0.4% SDS (w/w) (in ATP-containing homogenizing medium) and incubated an additional 10 min at room temperature. The detergent-treated microsomes were layered on top of a three-step sucrose gradient (all densities prepared in homogenizing medium) of 15, 25, and 45% and centrifuged in a swinging bucket rotor (Beckman SW-28) at 100000*g*, 2.5 h. The membrane fractions collected at the 25−45% interface were used for these experiments. Protein concentration was determined by the method of Lowry et al. (*23*) using BSA as standard.

Erythrocyte Membrane Preparation. Porcine blood was obtained from Pel-Freez Biologicals (Rogers, AR), and all blood processing was done on ice. Approximately 40 mL of heparinized whole blood was collected in a Beckman centrifuge tube (50 mL) and centrifuged for 5 min at 12000*g* and 4 °C (Beckman J2-21 centrifuge; JA-20 rotor). The blood plasma and buffy coat were removed by aspiration, and the remaining erythrocytes were washed three times with 165 mM NaCl. The erythrocytes were diluted 6-fold into a lysis medium containing 1 mM $MgCl_2$, 2 mM EGTA, and 5 mM Na_3PO_4 (pH 7.4) and stirred for 15 min on ice. The resulting solution was then centrifuged for 20 min at 27000*g* and 4 °C. The pellets were resuspended in lysis buffer and centrifuged for 15 min at 27000*g* and 4 °C. The resulting pellets were frozen and thawed twice. After each freeze/thaw cycle, the pellets were washed with lysis buffer and centrifuged at 27000*g* for 15 min at 4 °C (pellets were washed until supernatants were clear and pellets were light pink). The final pellets were combined and washed once in 20 mM Tris-HCl, pH 7.6. Erythrocyte membranes were frozen in 200 μL aliquots at −20 °C until needed. Protein content was determined by the method of Lowry (*23*) using BSA as standard (Lowry kit, Sigma-Aldrich, St. Louis, MO).

ATPase Measurements. For PMCA measurements, ATP hydrolysis was measured as reported previously for the red cell Ca pump (*24*), with minor modifications. Briefly, approximately 350 μg/mL protein from erythrocyte membranes was digested for 10 min on ice to remove the calmodulin sensitivity of the PMCA activity. The digestion solution contained 100 μM EGTA, 160 mM KCl, 17 mM Tris-HCl pH 7.4, and 5 μg/mL chymotrypsin. The digestion process was stopped with 6.5 μg/mL aprotinin.

PMCA activity experiments were performed on chymotrypsin-digested enzyme by measuring the liberation of $^{32}PO_4$ from $\gamma[^{32}P]$ATP. Specifically, 17.5 μg of enzyme (50 μL of enzyme in chymotryptic digestion solution) was diluted into 500 μL of an ATPase assay solution containing 15 mM MOPS/100 mM histidine pH 7.4 buffer, 110 mM NaCl, 3.55 mM ATP, 0.6 μCi/mL $\gamma[^{32}P]$ATP, 3.65 mM $MgCl_2$, 592 μM EGTA, and 6.5 μg/mL aprotinin. In experiments with saturating $[Ca^{2+}]$ (Figures 3, 5, 9, and 11B), free calcium was added to this assay solution at a final concentration of 0.277 μM (titrated with EGTA). In experiments that measured the Ca-dependence of activity (Figures 6 and 9B), the free calcium was varied by mixing Ca EGTA and EGTA solutions. (The final free calcium concentration in these assay mixtures was verified using Fura-2 fluorescence, with a K_d for Fura-2 of 0.14 μM.) Background measurements were performed with 592 μM EGTA and no calcium present in the assay solution. The assay mixture containing enzyme was incubated for 1 h at 37 °C. The reactions were stopped with the addition of 1 mL of an ice-cold solution containing 12 mM trichloroacetic acid and 100 mg/mL activated charcoal. The activated carbon binds organophosphates and is removed from the suspension by centrifugation in a microfuge at 4000 rpm for 2 min. A 0.5 mL volume of each supernatant containing unbound inorganic phosphate was assayed with liquid scintillation spectroscopy.

For Na,K-ATPase measurements, 0.1 mg quantity of purified canine renal sodium pump enzyme was diluted into 2.8 mL of 200 mM imidazole titrated to pH 7.4 with dilute HCl. This mixture was warmed at 37 °C for 10 min before 50 μL aliquots were diluted 12-fold into 550 μL of an assay solution containing 50 mM imidazole at pH 7.4, 10 mM $MgCl_2$, 0.5 mM TrisATP, 0.5 μCi $\gamma[^{32}P]$ATP, either 130 mM NaCl or 5 mM KCl, plus indicated inhibitor concentrations or Tris-HCl, pH 7.4 (as an ionic strength control). The quadruplicate samples were then incubated for 10 min at 37 °C (1 mM ouabain was included in quadruplicate samples containing either 1.5 mM KCl or 64 mM NaCl to give ouabain-insensitive pump activity). The reactions were stopped and liberated $^{32}PO_4$ determined as described above.

p-Nitrophenylphosphatase Activity. All pNPPase assays were conducted using 2−4 μg of Na,K-ATPase from dog kidney preparations. It is important to note our observation that the pNPPase activity was sensitive to the total salt concentration of the reaction medium, especially below 100 mM total salt (data not shown). Thus, we were careful to use buffered reaction media at (or greater than) 100 mM and also matched the concentration of inhibitor present with equal molar amounts of imidazole, Tris, MOPS, or choline. Besides an apparent ionic strength effect at low salt, none of these organic cations produced dose-dependent inhibition of pNPPase activity. In brief, the assay buffer contained 50 mM MOPS/Tris, 3 mM $MgCl_2$, pH 7.4 (unless otherwise indicated) with a final concentration of 5 mM di-tris pNPP and 100 mM choline-Cl (or other salt for ionic strength equilibration) for each reaction tube. For IC_{50} experiments, 2 mM K^+ was used while varying the concentrations of the quaternary amines over the range indicated in the figure legends. For K^+ competition experiments, the amount indicated in the figure legend of the quaternary amines was used while varying the concentration of K^+ over the indicated concentration range. Each reaction tube was incubated at 37 °C for 15 min and the reaction stopped by the addition of 200 μL of "ice-cold" 200 mM NaOH and the reaction tubes placed in an ice bath for 10 min. Absorbance at 410 nm was then recorded utilizing a Beckman DU-530 spectrophotometer and absorbance converted to activity based on a pNP standard curve.

Phosphorylation by γ[^{32}P]ATP. The amount of phosphoenzyme was determined similar to the methods reported previously (*25*). Briefly, we measured whether TMA or TEA would prevent phosphorylation from Na^+ and MgATP. For these experiments, chymotrypsin-treated enzyme was utilized. The chymotrypsin treatment was performed according to the method of Jorgensen and Farley (*26*). Dog kidney enzyme was digested for 15 min at 37 °C in a solution containing 1.7 mg/mL of purified Na,K pump, 0.1 mg/mL of chymotrypsin, 0.85 mM NaCl, 13 mM TrisHCl (pH 7.4), and 0.085 mM EDTA. The reaction was stopped by diluting the solution 23-fold into an ice-cold solution of 1 mM Na^+, 190 mM NMDG HEPES (pH 7.4) containing 0.4 mg/mL aprotinin. Enzyme phosphorylation was then determined by diluting this chymotrypsin-treated enzyme stock to approximately 10 μg/mL of protein with 144 mM *N*-methyl-D-glucamine, 1 mM NaCl, 3.5 mM $MgCl_2$, 35 mM Tris HCl, pH 7.5 and 10 μM γ[^{32}P]ATP in the presence or absence of inhibitor or potassium for 30 s on ice. The reaction was quenched by the addition of 60% trichloroacetic acid, 3 mM ATP, 6 mM Tris phosphate, filtered, and washed three times in the same solution. Each condition was assayed via liquid scintillation spectroscopy (in quadruplicate).

Modeling Procedures. The structures of the Na pump and PMCA were modeled based on the crystal structure of a homologous protein, Ca^{2+} pump (SERCA1a). The Ca^{2+}-free thapsigargin bound conformation (PDB code: 1IWO) was used as the template (*10*, *27*). The rationale for this choice is provided in Results. The sequence alignment by Sweadner and Donnet (*28*) was adopted for the Na pump homology modeling and a BLAST alignment for PMCA homology modeling (*29*−*31*). The three-dimensional structure was constructed using the Modeler program (*32*) after removing the bound thapsigargin and allowing the protein to "relax". The constructed pump models were further optimized via AMBER force field minimization (*33*) to remove bad clashes. (Bad clashes refer to distances too close between nonbonded atoms that lead to strong van der Waals repulsion.) After optimization, most bad clashes were removed from the modeled structure. The remaining bad clashes were located either far from the cation binding site (for both pumps) or within the large PMCA insert, and therefore had little effect on the modeling calculations. Hydrogen atoms were added, and atomic charges and types were assigned via Sybyl (Tripos, Inc.).

The atomic coordinates of the organic cations were obtained from the Cambridge Structural Database (CSD, a database consisting of crystal structures of small organic compounds; *34*). Atom types were assigned and Gasteiger atomic charges were loaded using Sybyl. All molecular graphics images were produced using the MidasPlus program (*35*).

Molecular Modeling on the Pumps with DOCK. DOCK 4.0 (*36*) was used to generate feasible binding orientations and to estimate binding tightness around the interesting sites on the Na pump and PMCA. We focused on the regions surrounded by Segments M1, M2, M3, M4 and the P domain. The molecular surface of the pump was generated using the *dms* program provided by MidasPlus (*35*). The negative image of the surface, consisting of the DOCK sphere points, was created by using the program SPHGEN of the DOCK software for future matching with the ligand atoms. Around 60 sphere points were selected, representing putative ligand positions. For each ligand molecule, docking was initially performed to generate possible ligand orientations, with "maximum_orientations" set to 500, "grid_spacing" set to 0.3 Å, "scoring_function" set to the force field scoring function, and "energy_cutoff" set to 10 Å. The generated 500 orientations were further optimized with a generalized-Born type (GB) energy function, consisting of an electrostatic energy component accounting for the water effect and a 6−12 Lennard-Jones van der Waals (VDW) energy component (*37*, *38*). The best orientation is the orientation with the lowest GB energy score.

The effect of protein flexibility was investigated by performing energy minimization for the Na pump (with or without TMG) and the docked ligand via Amber force field, which allows both the protein and the ligand to have limited conformational changes. These control modeling experiments revealed no significant changes for ligand binding scores before and after minimization. Large protein conformational changes are beyond our modeling ability.

RESULTS

In these studies, we investigated the inhibition of a series of three different types of organic cations, (i) guanidines, (ii) quaternary amines, and (iii) diamines (Figure 2). The main focus was to determine whether these inhibitors bound to the inside facing the cation site to block Ca or Na pump function.

We measured PMCA and Na pump function, concentrating on properties of cytoplasmic cation activation. For the Ca pump, we measured Ca^{2+}-stimulated ATPase activity and also the Ca^{2+}-dependence of inhibition to determine if the inhibitor cations competed with Ca^{2+} at the cytoplasmic site. For the Na pump, we tested both ATPase and pNPPase activity. Na^+-activation of ATPase takes place at the internal site, and K^+-activation of pNPPase also takes place at the internal site. Our approach was based upon a simple kinetic model (Figure 1), which has inherent predictions on the behavior of alkali metal mimicking inhibitors (*39*). For example, an inhibitor, I, that binds to the transport site solely from the inside would compete with Na for Na,K-ATPase and *K* for pNPPase activity on the Na pump; likewise, it would compete with Ca^{2+} for PMCA ATPase activity. An additional prediction is that inhibitor I would compete with Na^+ to block Na pump phosphorylation in the forward direction from Na^+, Mg^{2+}, ATP. Such an approach provides clear delineation between inside and outside effects, without the need for a sided preparation. Also to avoid concerns about interactions with calmodulin, red cell membranes were treated with chymotrypsin to remove the calmodulin binding autoinhibitory region on PMCA.

Quaternary Amines. PMCA. Interestingly, none of the quaternary amines (QA) inhibited PMCA (Figure 3). The inability of quaternary amines to block PMCA cannot be because PMCA excludes monovalent organic cations, since below we show that a different class of monovalent organic cation does inhibit PMCA (see guanidines).

Na Pump. The ability of tetramethyl, tetraethyl, and tetrapropyl ammonium to inhibit the Na pump was determined by measuring different modes of Na pump activity. In contrast to PMCA, TPA inhibited the Na pump pNPPase

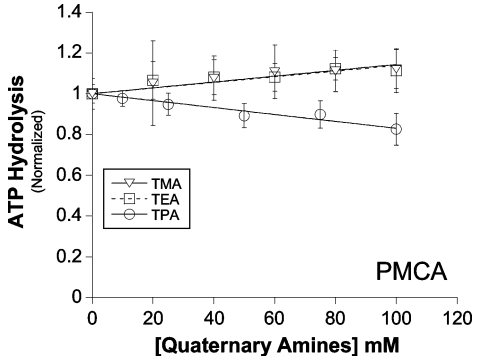

FIGURE 3: Dose-dependent inhibition of plasma membrane Ca-ATPase by quaternary ammonium compounds. Calcium-dependent ATPase activity of PMCA from porcine red cell membrane preparations was measured as described in Methods in the presence of the indicated concentrations of TMA, TEA, or TPA. None of these compounds were able to effectively reduce PMCA activity. Even at 100 mM TPA, less than 10% inhibition was observed. The data from at least three different experiments were normalized to Ca^{2+}-dependent ATPase activity in the absence of inhibitor. Points represent means ± SEM.

activity, whereas TMA and TEA did not inhibit (Figure 4). Initial examination of QA inhibition of pNPPase activity suggested that only TPA (not TEA or TMA) was able to inhibit the Na pump (Figure 4A); however, in other assays we found that TEA was also able to inhibit the Na pump. By examining the cation-dependence of QA inhibition of various Na pump reactions, we determined the sidedness of the interaction. Not surprisingly, we observed that TEA could inhibit from the outside as its inhibition was competitive with K^+ (Figure 4B) for activation of ATPase activity. Interestingly, we also found that TEA could inhibit from the cytoplasmic side because it could block EP formation from Na, Mg, and ATP (Figure 4C). In these experiments, the Na,K-ATPase was treated with chymotrypsin to prevent the conformational change from ADP-sensitive to K^+-sensitive EP (*26*). In contrast, although TPA is an effective inhibitor of the Na pump, we recently showed that TPA is absolutely excluded from the cytoplasmic cation site (*40*). In this earlier study we also showed the inability of TMA to inhibit EP formation in the Na pump (*40*).

Guanidines. PMCA. GUA and TMG inhibited the Ca^{2+}-dependent ATPase activity of PMCA (Figure 5). A simple one-site inhibition model did not fit the data very well. The one site inhibition equation was $v(I) = v(0)IC_{50}/(IC_{50} + I)$, where $v(I)$ is the activity in the presence of inhibitor, $v(0)$ is the activity in the absence of inhibitor, I is the inhibitor concentration, and IC_{50} is the inhibitor concentration for an activity of $v(0)/2$. The data were better fit by cooperative binding of two guanidine molecules using the equation, $v(I) = v(0)IC_{50}^2/(IC_{50}^2 + I^2)$. The IC_{50} values for PMCA inhibition were 51 ± 3 mM and 19 ± 3 mM for GUA and TMG, respectively (Figure 5, $R > 0.99$). Figure 6 shows that guanidine competed with Ca^{2+} to inhibit PMCA; these data are most easily explained by GUA binding to the cytoplasmic cation site and preventing Ca^{2+} binding.

Na Pump. Figure 7 shows the inhibition of Na,K-ATPase activity by GUA and TMG. Again, these data were not well fitted with a simple one site inhibition model ($R = 0.93$); rather the data were much better fit by the equation: $v(I) = v(0)IC_{50}^2/(IC_{50}^2 + I^2)$, ($R = 0.99$). This is consistent with more than one GUA or TMG molecule binding to the Na

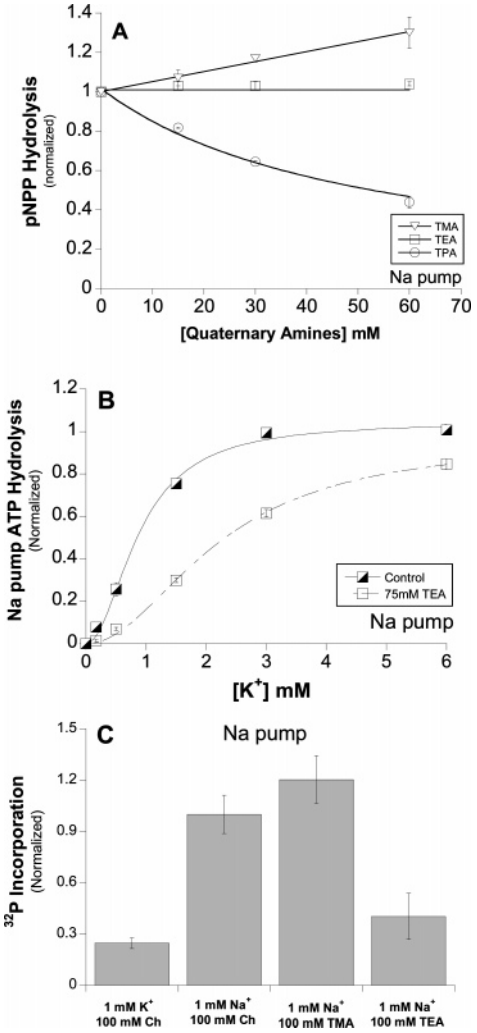

FIGURE 4: Tetraethylammonium inhibition of Na pump. (A) Ouabain-sensitive pNPPase activity of Na,K-ATPase purified from dog kidney was measured as described in Methods in the presence of the indicated concentrations of TMA, TEA, and TPA. Neither TMA nor TEA decreased pNPPase activity, whereas TPA inhibited with an IC_{50} of 51 ± 5.9 mM. (B) The K^+ concentration-dependence of inhibition of ATPase activity was measured in the presence of saturating substrates. The presence of 75 mM TEA increased the K_m for K^+, while V_{max} was not significantly different from control (i.e., 75 mM Tris), consistent with competition. Control: V_{max} = 1.05 ± 0.02, K_m = 0.89 ± 0.06; TEA: V_{max}= 0.96 ± 0.02, K_m = 2.22 ± 0.08. Points represent means ± SEM. Data were fit to the Michaelis−Menten equation with an S^2 term to represent that more than one K^+ ion binds, producing the sigmoidicity observed. (C) Effect of TMA and TEA on phosphoenzyme formation. Purified Na,K-ATPase was treated with chymotrypsin to prevent the conformational switch to K^+-sensitive EP and phosphorylated as described in Methods in the presence of the indicated cations. A 100 mM concentration of TEA significantly reduced EP levels, where 100 mM TMA was not different from the positive control. These data are consistent with TEA binding to the inside facing cation site. Data are from three experiments of quadruplicate determinations and normalized to the level of EP formed in the presence of 1 mM Na^+, 100 mM choline-Cl. Background phosphorylation is shown in the first bar (1 mM K^+, 100 mM choline-Cl). Bars represent means ± SEM.

pump. The IC_{50} values were 188 ± 3 mM for GUA and 31 ± 2 mM for TMG.

The presence of either GUA or TMG increased the K_m for Na^+ and slightly decreased V_{max} for ATPase activity (Figure 8A). Similarly, these compounds increased the K_m for K^+, and slightly decreased V_{max} for pNPPase activity

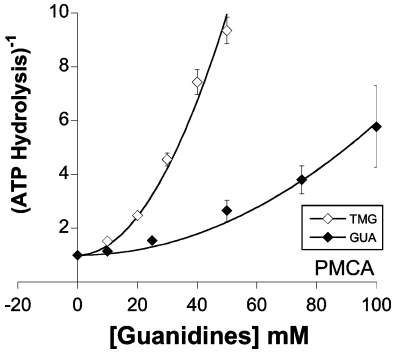

FIGURE 5: Dose-dependent inhibition of plasma membrane Ca-ATPase by guanidines. Calcium-dependent ATPase activity of PMCA from porcine red cell membrane preparations was measured as described in Methods in the presence of the indicated concentrations of guanidine (GUA) or tetramethylguanidine (TMG). Both chemicals demonstrate a dose-dependent inhibition of the calcium pump and the data were fit to the equation: $v(I) = v(0)IC_{50}^2/(IC_{50}^2 + I^2)$ (see Results) (IC_{50} values for GUA and TMG were 51 ± 3 mM and 19 ± 3 mM, respectively). Inhibition of PMCA required a squared term in the IC_{50} equation (see Results). In each case, saturating quantities of Ca^{2+}, Mg^{2+}, and ATP were used. The data from at least three different experiments were normalized to ATPase activity in the absence of inhibitor. Points represent means ± SEM.

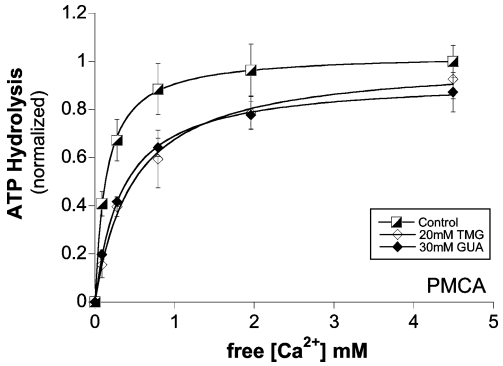

FIGURE 6: Guanidines compete with Ca for the cytoplasmic cation site on the PMCA. Ca^{2+}-activation of ATPase activity was measured in the presence of saturating substrates. Increasing concentrations of Ca^{2+} in the presence of 30 mM guanidine (GUA) or 20 mM tetramethyl-guanidine (TMG) increased the K_m for Ca^{2+} (to 0.34 ± 0.015 μM and 0.48 ± 0.05 μM, respectively) compared to control K_m (0.138 ± 0.005 μM) in the absence of inhibitor. The significant increase in the K_m and extrapolation to the same V_{max} is consistent with GUA and TMG competing with Ca^{2+} at the cytoplasmic site. The data for each curve were normalized triplicate determinations from a single experiment representative of at least three different experiments. Points represent means ± SEM.

(Figure 8B). Both of these observations are consistent with guanidines competing with the binding of Na^+ or K^+, respectively, to the cytoplasmic cation site. It is important to note that at higher concentrations both GUA and TMG appear to be more mixed-type inhibitors rather than pure competitive inhibitors (Figure 8), which resulted in the inability to fully attain control V_{max} levels in the presence of GUA or TMG. The appearance of mixed-type inhibition at higher concentrations is likely because at these concentrations guanidines can also inhibit from the extracellular side (*41*). But the binding constants are substantially better for these guanidines binding to the inside than to the outside.

When the level of phosphoenzyme (EP) was measured in the presence of 1 mM Na^+, the addition of 40 mM GUA produced a dramatic reduction in the steady-state EP level. Moreover, increasing the [Na^+] significantly retarded the

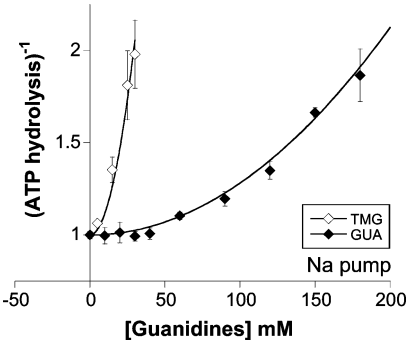

FIGURE 7: Dose-dependent inhibition of Na,K-ATPase by guanidines. Ouabain-sensitive ATPase activity of Na,K-ATPase purified from dog kidney was measured as described in Methods in the presence of the indicated concentrations of guanidine (GUA) or tetramethylguanidine (TMG). Both chemicals demonstrate a dose-dependent inhibition of the sodium pump (IC_{50} values for GUA and TMG were 188 ± 3 mM and 31 ± 2 mM, respectively). Data for both compounds required a squared term in the IC_{50} equation (see Results), consistent with more than one inhibitor molecule binding to the pump. In each case saturating quantities of Na^+, K^+, Mg^{2+}, and ATP were used. The data from at least three different experiments were normalized to ATPase activity in the absence of inhibitor. Points represent means ± SEM.

ability of GUA to prevent EP formation (data not shown). Taken together, these data are consistent with GUA binding to the inside facing cation site in a mutually exclusive manner with Na^+ ions.

Although the IC_{50} for guanidine inhibition of PMCA is substantially less than observed for the Na pump, it is not fair to compare the IC_{50} values because the substrate concentrations (Ca^{2+} vs Na^+ for PMCA and Na^+ pump, respectively) are not the same fraction of K_m in the two cases. Thus, it is more appropriate to compare K_i values between pumps, i.e., via the relationship $Km_{app} = K_m(1 + I/K_i)$ in the presence of inhibitor. Using this equation, we calculated a K_i for inhibition for the two pumps. Interestingly, the K_i values for GUA are quite similar for the two pumps with values of ~16 mM and ~10 mM for the Na pump and PMCA, respectively.

Alkyl Diamines. PMCA. Alkyl diamines inhibited PMCA. Propyl diamine was clearly the best inhibitor, and ethyl and butyl were both weak inhibitors (Figure 9). Propyl diamine inhibition was best fit with a model with two binding sites. Interestingly, ethyl diamine did not compete with Ca^{2+} on PMCA (Figure 9B). Propyl diamine increased K_m about 4-fold with perhaps a slight (10%) effect on V_{max}, suggesting that the primary effect of propyl diamine is by competition with Ca^{2+} on the PMCA (Figure 9B).

Na Pump. The IC_{50} curves for ethyl, propyl, and butyl diamine inhibition of Na pump pNPPase activity are shown in Figure 10. Interestingly, based upon the *R* values, the diamine inhibition curves for Na pump pNPPase appeared to be fit equally well by equations with Hill coefficient $n = 1$ or $n = 2$. Yet, neither fit was satisfying when one looked at the resulting curves in relation to the data. Rather, the data seemed best fit by an equation that accommodated the binding of two inhibitor molecules with different apparent affinities (K_{d1} and K_{d2}), which compete with substrate (S) binding $v = A/(B + K_{d2} * I + I^2)$, where v is the reaction velocity, $A = V_{max}[S](K_{d1}K_{d2}/K_m)$ and $B = K_{d1}K_{d2}(1/[S]/K_m)$. The inhibitory potency of ethyl and propyl diamine appeared similar, whereas the larger butyl diamine was about 5-fold

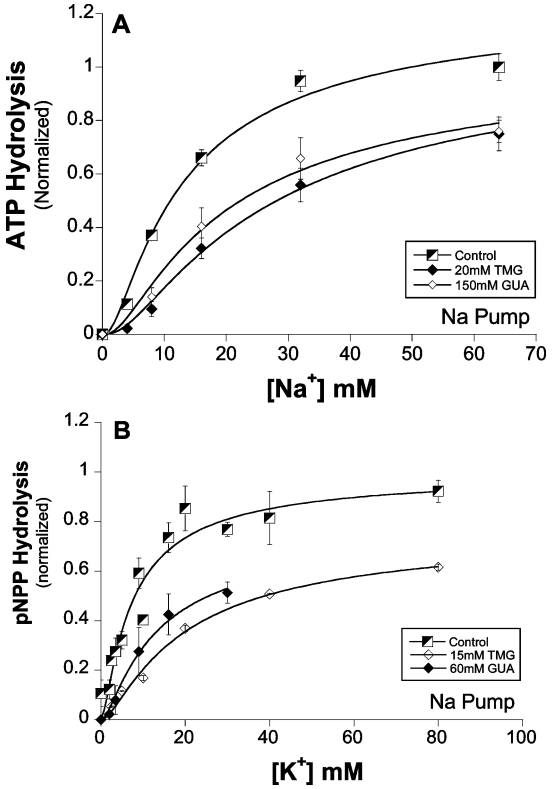

FIGURE 8: Guanidines compete with Na and K for the cytoplasmic cation site on the Na pump. Na-activation of ATPase activity was measured in the presence of saturating substrates. (A) Increasing concentrations of Na^+ in the presence of 150 mM GUA or 20 mM TMG decreased the inhibitory efficiency for both guanidines consistent with competition. Notably, the K_m for Na^+ increased by approximately 3-fold with guanidines present compared to control K_m. V_{max} values were control: 1.26 ± 0.07; GUA: 1.11 ± 0.05; TMG: 1.04 ± 0.08. (B) In a similar fashion, the K^+-activation of pNPPase activity was measured in the presence of either 60 mM GUA or 15 mM TMG. Again the presence of either GUA or TMG substantially increased the K_m for K^+ 2−3-fold. V_{max} values were control: 0.99 ± 0.07; GUA: 0.77 ± 0.06; TMG: 0.77 ± 0.04. The significant increase in the K_m for both ATPase and pNPPase activity is consistent with GUA and TMG competing with the endogenous cation at the cytoplasmic site. The data for each graph were normalized triplicate determinations from a single experiment representative of at least three different experiments. Points represent means ± SEM.

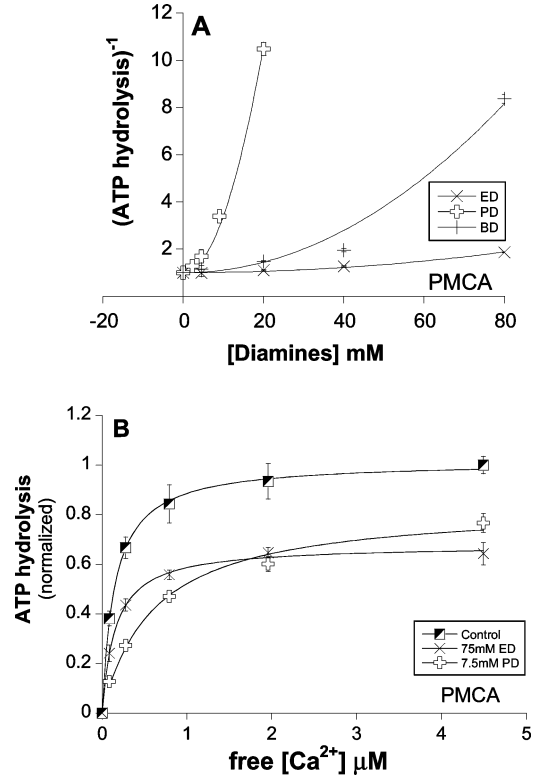

FIGURE 9: Alkyl diamine inhibition of PMCA. (A) Concentration-dependence of Ca-ATPase inhibition by ethyl (ED), propyl (PD), and butyl (BD) diamine. Experiments were performed as in Figure 3; the data were fit to the equation: $v(I) = v(0)IC_{50}^2/(IC_{50}^2 + I^2)$ (see Results) and the IC_{50} values were 88 ± 3 mM for ED, 7 ± 1 mM for PD, and 27 ± 5 mM for BD. (B) Ca^{2+}-activation of chymotrypsin-treated PMCA activity was measured in the presence of (in mM) 0.6 $MgCl_2$, 0.5 ATP, 0.462 EGTA, 15 MOPS, and 100 histidine. Increasing concentrations of Ca^{2+} in the presence of 75 mM ED were unable to displace ED and attain control V_{max} levels. Control V_{max} = 1.02 ± 0.01, K_m = 0.14 ± 0.01 μM; ED V_{max} = 0.68 ± 0.01, K_m = 0.16 ± 0.01 μM. In contrast, Ca^{2+} and PD appear to compete. Increasing concentrations of Ca^{2+} in the presence of 7.5 mM PD were able to displace PD and attain control V_{max} levels. Control, PD V_{max} = 0.85 ± 0.04, K_m = 0.61 ± 0.1 μM. The data from at least three different experiments were normalized to Ca^{2+}-dependent ATPase activity in the absence of inhibitor. Points represent means ± SEM.

less efficient, in contrast to the result on PMCA where propyl diamine was clearly better than either the smaller ethyl or the larger butyl diamine. Further investigation into the mode of Na pump inhibition by diamines shows that they preferentially bind to the cytoplasmic facing cation site as evidenced by competition with K^+ ions for pNPPase activity but not for Na,K-ATPase (Figure 10B,C).

pH Effect of Diamine Inhibition. Considering that diamines have two titratable nitrogen atoms, it was possible that inhibitory differences between these compounds were not only influenced by size but also by whether they had a +1 or +2 charge. Thus, the concentration dependence of diamine inhibition was repeated for both pumps at two separate proton concentrations. It was found that an increase in protons significantly increased the potency for ethyl diamine for both the Na pump and PMCA (Figure 11A,B). By itself, this observation is consistent with either protons titrating ethyl diamine, increasing its charge from +1 to +2 or with protons titrating a residue on the sodium pump, increasing the affinity for diamines. Interestingly, propyl diamine inhibition of PMCA was unaffected by increased protons (Figure 11B). For the Na pump, propyl diamine inhibited less well at low pH. Over this pH range, propyl diamine should always be +2 charged, and therefore the decrease in pH from 7.4 to 6.8 would not affect the state of propyl diamine. Since there was no change in PMCA inhibition with propyl diamine, our results are consistent with the increased inhibition by ethyl diamine being the result of titration of ethyl diamine and not of the pump. For the Na pump, our results are consistent with both ethyl diamine and the Na pump being titrated. Specifically, the increased ethyl diamine inhibition was the result of titration of ethyl diamine, whereas the apparent affinity for propyl diamine decreased (Figure 11A). Since propyl diamine is completely titrated within this pH range, the decreased affinity must be due to a change in the Na pump.

Molecular Modeling. To interpret the consequences of the experimental data in terms of pump mechanism, both kinetic and structural implications need to be considered. Thus, we

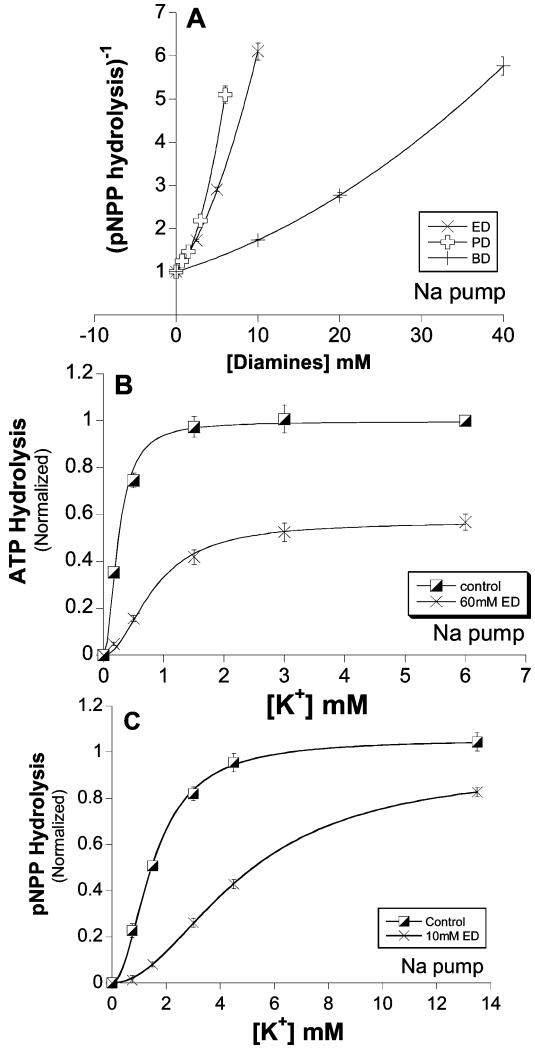

FIGURE 10: Alkyl diamine inhibition of Na^+ pump. (A) Concentration-dependence of pNPPase inhibition by ethyl (ED), propyl (PD), and butyl (BD) diamine. Experiments were performed as in Figure 4A; the data were fit to the equation: $v = A/(B + K_{d2} * I + I^2)$ (see Results) and the extrapolated apparent affinities for the two binding sites, K_{d1} and K_{d2} were 2.5 and 6.9 mM for ED, 1.2 and 3.5 mM for PD, and 38.5 and 51.5 mM for BD. (B) K^+-activation of Na,K-ATPase activity was measured in the presence of 20 mM $MgCl_2$, 3 mM ATP, and 50 mM NaCl. Increasing concentrations of K^+ in the presence of 60 mM ED were unable to displace ED and attain control V_{max} levels. Control V_{max}= 1.00 ± 0.02, K_m = 0.25 ± 0.017 mM; ED V_{max} = 0.57 ± 0.02, K_m = 0.84 ± 0.056 mM. (C) K^+-activation of pNPPase activity was measured in the presence of 3 mM $MgCl_2$, 5 mM pNPP, 50 mM MOPS/Tris, and 100 mM choline-Cl. Increasing concentrations of K^+ in the presence of 10 mM ED were able to displace ED and attain control V_{max} levels. Control V_{max}= 1.05 ± 0.02, K_m = 1.5 ± 0.04 mM; ED V_{max} = 0.93 ± 0.02, K_m = 4.9 ± 0.06 mM. The data from at least three different experiments were normalized to ouabain-sensitive ATPase activity in the absence of diamine. Points represent means ± SEM.

constructed homology models for the Na pump and PMCA based upon the SERCA crystal structures. Such models would allow us to determine if there was a plausible structural model to accommodate our data, just as one might expect a plausible kinetic model to be presented to explain experimental observations. There are two difficulties with creating these homology models. First, what is the best sequence alignment? Second, which crystal structure do we choose?

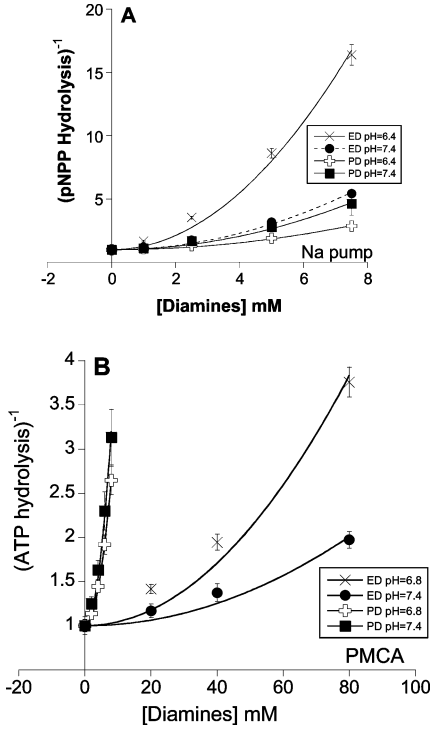

FIGURE 11: pH dependence of alkyl diamine inhibition of Na^+ pump and PMCA. (A) Ouabain-sensitive pNPPase was measured as described in Methods in the presence of the indicated concentrations of ethyl diamine (ED), or propyl diamine (PD). Filled symbols reflect experiments performed at pH = 7.4, whereas the "*X*" or "+" symbols reflect experiments at pH = 6.4. Both chemicals demonstrate a dose-dependent inhibition of pNPPase activity. The 10-fold increase in $[H^+]$ significantly increased the efficacy of ED; in contrast it slightly decreased the efficacy of PD. (B) PMCA activity was measured as described in Methods in the presence of the indicated concentrations of ED and PD. Filled symbols reflect experiments performed at pH = 7.4, whereas the "*X*" or "+" symbols reflect experiments at pH = 6.8. Similar to Na pump inhibition, the decrease in pH increased the efficacy of ED. The data from at least three different experiments were normalized to ATPase activity in the absence of inhibitor. Points represent means ± SEM.

We did sequence alignment for the Na pump and PMCA using two different programs, BLAST (*29*) and SPEM (*42*). The results were similar. We therefore decided to use the BLAST alignment of Sweadner and Donnet (*28*) for the Na pump and a BLAST alignment for PMCA. The alignment for PMCA is shown in Figure 12. For the Na pump, the homology and the alignment for the cytoplasmic cation access pathways and transport sites seem pretty reasonable. For PMCA, there is a large insert in this region (i.e., E^{294}–E^{348}) and not a lot of clear homology (cf. the homology models of ref *42*). However, Pinto and Adamo (*43*) have shown that deletion of this insert does not drastically alter PMCA function.

After aligning the pumps, we searched for the appropriate SERCA structures to build up the structures of PMCA and the Na pump. Unfortunately, we are interested in the structure of the pump when the transport sites are empty and accessible to the inside and to date SERCA has not been crystallized in this conformation. In the kinetic cycle, the two conformations that are closest are the occluded Ca^{2+} conformation (PDB code: 1SU4, formerly named 1EUL) and the thapsigargin bound conformation which is thought to have protons occluded (PDP code: 1IWO). We examined both conforma-

```
5   HSKSTEECLAYFGVSETTGLT--PDQVKRHLEKYGHNELPAEEGKSLWELVIEQFEDLLV 62   SERCA
47  HYGGVQNLCSRLKTSPVEGLSGNPADLEKRRQVFGHNVIPPKKPKTFLELVWEALQDVTL 106  PMCA

63  RILLLAACISFVLAWF-----------------EEGEETITAFVEPFVILLILIANAIVG 105
107 IILEIAAIISLVLSFYRPAGEENELCGQVATTPEDENEAQAGWIEGAAILFSVIIVVLVT 166

106 VWQERNAENAIEALKEYEPEMGKVYRADRKSVQRIKARDIVPGDIVEVAVGDKVPADIRI 165
167 AFNDWSKEKQFRGLQCRIEQEQKFSIIRNGQLIQLPVAEIVVGDIAQVKYGDLLPADG-- 224

166 LSIKSTTLRVDQSILTGESVSVIKHTEPVPDPRAVNQDKKNMLFSGTNIAAGKALGIVAT 225
225 ILIQGNDLKIDESSLTGESDHVKK-----------SLDKDPMLLSGTHVMEGSGRMVVTA 273

226 TGVSTEIGKIRDQMAATEQD---------------------------------------- 245
274 VGVNSQTGIIILTLLGVNEDDEGEKKKKGKKQGVPENRNKAKTQDGVALEIQPLNSQEGID 333

246 ---------------KTPLQQKLDEFGEQLSKVISLICVAVWLINIGHF---NDPVHGGS 287
334 NEEKDKKAVKVPKKEKSVLQGKLTRLAVQIGKAGLLMSALTVFILILYFVIDNFVINRRP 393

288 W--------IRGAIYYFKIAVALAVAAIPEGLPAVITTCLALGTRRMAKKNAIVRSLPSV 339
394 WLPECTPIYIQYFVKFFIIGITVLVVAVPEGLPLAVTISLAYSVKKMMKDNNLVRHLDAC 453

340 ETLGCTSVICSDKTGTLTTNQMSVCKMFIIDKVDGDFCSLNEFSITGSTYAPEGEVLKND 399
454 ETMGNATAICSDKTGTLTMNRMTVVQAYI-----------------GGIHYRQ---IPSP 493

400 KPIRSGQFDGLVELATICALCNDSSLDFNETKGVYEKVGEATETALTTLVEKMNVFNTEV 459
494 DVFLPKVLDLIVNGISINSAYTSKILPPEKEGGLPRQVGNKTECALLGFVTDLKQDYQAV 553

460 RNLSKVERANACNSVIRQLMKKEFTLEFSRDRKSMSVYCSPAKSSRAAVGNKMFVKGAPE 519
554 RN-----------EVPEEKLYKVYT--FNSVRKSMSTVIRNPNG-----GFRMYSKGASE 595

520 GVIDRCNYV--RVGTTRVPMTGPVKEKILSVIKEWGTGRDTLRCLALATRDTPPKREEMV 577
596 IILRKCNRILDRKGEA-VPFKNKDRDDMVRTVIE-PMACDGLRTICIAYRD--------- 644

578 LDDSSRFMEYE----TDLTFVGVVGMLDPPRKEVMGSIQLCRDAGIRVIMITGDNKGTAI 633
645 FDDTEPSWDNENEILTELTCIAVVGIEDPVRPEVPDAIAKCKQAGITVRMVTGDNINTAR 704

634 AICRRIGIFGENEEVADRAYTGREFDDLPLAEQREACRRAC--------CFARVEPSHKS 685
705 AIATKCGILTPGDDFL--CLEGKEFNRLIRNEKGEVEQEKLDKIWPKLRVLARSSPTDKH 762

686 KIVEYL-----QSYDEITAMTGDGVNDAPALKKAEIGIAMG-SGTAVAKTASEMVLADDN 739
763 TLVKGIIDSTVGEHRQVVAVTGDGTNDGPALKKADVGFAMGIAGTDVAKEASDIILTDDN 822

740 FSTIVAAVEEGRAIYNNMKQFIRYLISSNVGEVVCIFLTAALGLPEALIPVQLLWVNLVT 799
823 FTSIVKAVMWGRNVYDSISKFLQFQLTVNVVAVIVAFTGACITQDSPLKAVQMLWVNLIM 882

800 DGLPATALGFNPPDLDIMDRPPRSPKEPLIS 830
883 DTFASLALATEPPTESLLKRRPYGRNKPLIS 913
```

FIGURE 12: The sequence alignment between SERCA and PMCA by the BLAST program. For each alignment row, the upper line is the SERCA sequence and the lower line is PMCA. The Na pump was aligned according to that of Sweadner and Donnet (*28*). The "*" symbols represent identical amino acid residues, whereas, the ":" symbols show residue pairs with positive matrix scores, representing similar sequence alignment according to the BLAST algorithm.

tions. In the 1SU4 structure, the putative Ca^{2+} access region is closed because of the extension of TM1, leaving not enough room for ligand binding. The 1IWO structure provided the best fit to the data; thapsigargin was removed since it does not bind to these two pumps. The structure around the thapsigargin was allowed some flexibility and clashes and inserts were adjusted by AMBER force field minimization in Sybyl.

The present investigation was to find out whether these models are consistent with organic cations binding to these pumps. These molecules were individually docked into the region enclosed by M1, M2, M3, M4, and the P domain. Energy efficiency of binding was used to predict the preference of inhibitor binding to these pumps.

Figure 13 shows the top 100 orientations for tetramethylguanidine binding to the cytoplasmic access region of the Na pump. The best orientation of TMG is shown in dark blue in Figure 14A, binding to a site surrounded by M3 (yellow), M4 (yellow-green), and the P domain (cyan). We also investigated the possibility of binding a second ligand to the intracellular side of the pump. Again, TMG was used as an example. The best orientation of TMG (blue molecule

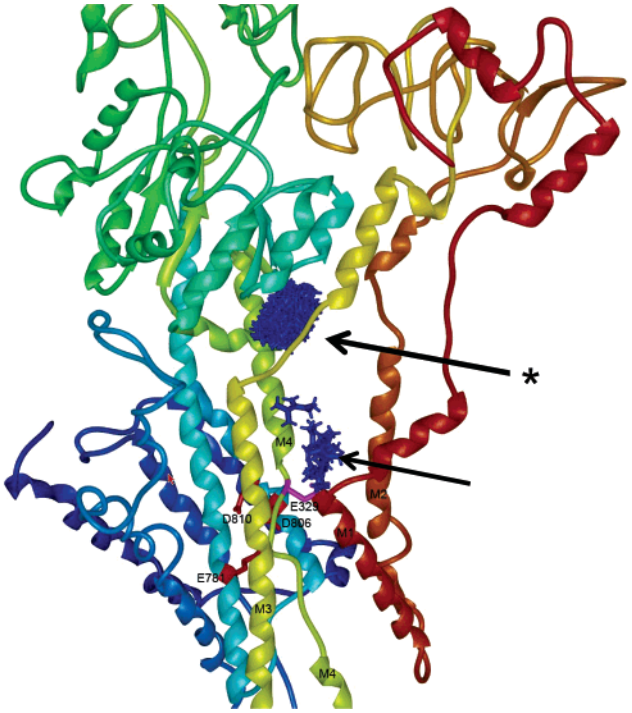

FIGURE 13: The Na pump has two predicted cytoplasmic TMG binding sites. Homology model of the Na,K-ATPase aligned to the high-resolution SERCA structure (PDB code: 1IWO). The pump is represented in ribbon form (red to blue from N- to C-terminus). Five-hundred molecules of TMG were placed within the model via the DOCK 4.0 program and minimized based on an energy scoring function of VDW and electrostatic interactions. Then the 500 docked orientations were re-ranked via energy minimization with a GB energy scoring function; only the top 100 orientations are shown in the figure. These 100 molecules formed two clusters seen at the tips of the arrows. The * indicates the site that ranked highest. Acidic residues are red except E^{329} (in magenta).

in Figure 14A, located in site 1 coordinated by D^{724} and D^{742}) was chosen as the first bound ligand and was treated as part of the pump in later modeling calculations. A second TMG molecule was then docked to the Na pump (site 2; Figure 14A). There are three possible binding sites for the second TMG (designated a, b, and c, Figure 14A) according to computer-generated binding energy efficiency, with site 2a (coordinated by E^{284} and E^{357}) and 2b (coordinated by E^{284} and E^{329}) slightly more likely than site 2c (coordinated by E^{146} and E^{154}). The three potential binding modes for the second TMG are simultaneously shown in light-blue color (Figure 14A). Models generated for the binding of GUA to the Na pump suggested that like TMG, two molecules of GUA bind preferentially from the cytoplasm (data not shown). Thus, we can develop a plausible structural model of the Na pump that accommodates two TMG molecules, even though this structural model is not based upon the "correct" kinetic conformation; a crystal structure for any pump which has the transport site empty and cytoplasmically accessible does not yet exist.

The binding of tetramethylguanidine was also modeled with PMCA (Figure 14B,C). One striking difference between PMCA and the Na pump (and SERCA) is a large insertion in the cytoplasmic access region (colored gray, Figure 14B,C). Given the finding that the deletion of this insert does not dramatically alter PMCA function (*43*), we chose to do our docking calculations by removing this insert from the pump, although this insert (gray) is shown in Figure 14B,C for completeness.

Even though the negative charges that form site 1 for the Na pump are present in PMCA, we chose the conservative approach of looking for other sites that might also bind TMG or guanidine as the insert might block access to site 1. Indeed, tetramethylguanidine and guanidine appear able to bind near the access gate Glu-423 (equivalent to E^{309} in SERCA), roughly comparable to site 2b in the Na pump (Figure 14A). In addition, there was a second site to which TMG or GUA could bind (site B, Figure 14B). In contrast, energy efficiency measurements indicated that the preferred site of ethyl diamine binding is at a site away from the access glutamate (site C, Figure 14C). It appears that ethyl diamine is too small to make strong contacts with residues which coordinate sites A or B in the PMCA structure (Figure 14C). Thus, like the Na pump, we can develop a plausible structural model of PMCA that accommodates two TMG molecules, even though there is a large insertion near this region (again the kinetically equivalent conformation, inside open and empty, has not yet been crystallized for any P-type pump).

The docking calculations of the quaternary amines (QAs, i.e., TMA, TEA, and TPA) to the cytoplasmic access region of the Na pump were also performed. While TPA can bind in the access region, it is so large that the entrance path (enclosed by segments M1, M2, and M3) is extremely tight for TPA (see Figure 15). Because of its bulk, TPA is required to keep changing its orientation along the entrance path to avoid steric collision with the Na pump, which is entropically unfavorable. Size is not a restriction for the much smaller TMA and TEA. However, TMA is too small to make adequate contacts for stable coordination. TEA appears to fit, but the modeling gave a poor energy score at the potential binding site. Thus, the homology model is consistent with the size selectivity for quaternary amines so this model of the region around the access area is consistent with the experimental results.

Very recently, a refined crystal structure has been solved for the SERCA E2 conformation by Toyoshima and colleagues (PDB 2AGV, *44*). One striking difference between 2AGV and 1IWO (the previously published SERCA E2 conformation) is that the side chain of E^{309} points outside in 1IWO but inward in 2AGV. To examine the robustness of our predictions, we also modeled the Na pump and PMCA structures based on the new template 2AGV and repeated all the docking calculations. The results are not significantly different from those obtained using the 1IWO template, suggesting that our predictions are robust and reliable. The 1IWO structure provides slightly better fit to the experimental data than the 2AGV structure.

DISCUSSION

In this paper, we determined some key characteristics for P-type pump inhibition by organic cations. Not surprisingly, monovalent quaternary amines did not inhibit the PMCA. Quaternary amine effects on Na pump were size dependent: the smallest, TMA, not inhibiting at all, the largest, TPA, only inhibiting from the outside, and TEA able to inhibit from both sides. Interestingly, guanidine and tetramethylguanidine inhibited both pumps about equally well; on the Na pump they inhibited inside much better than outside.

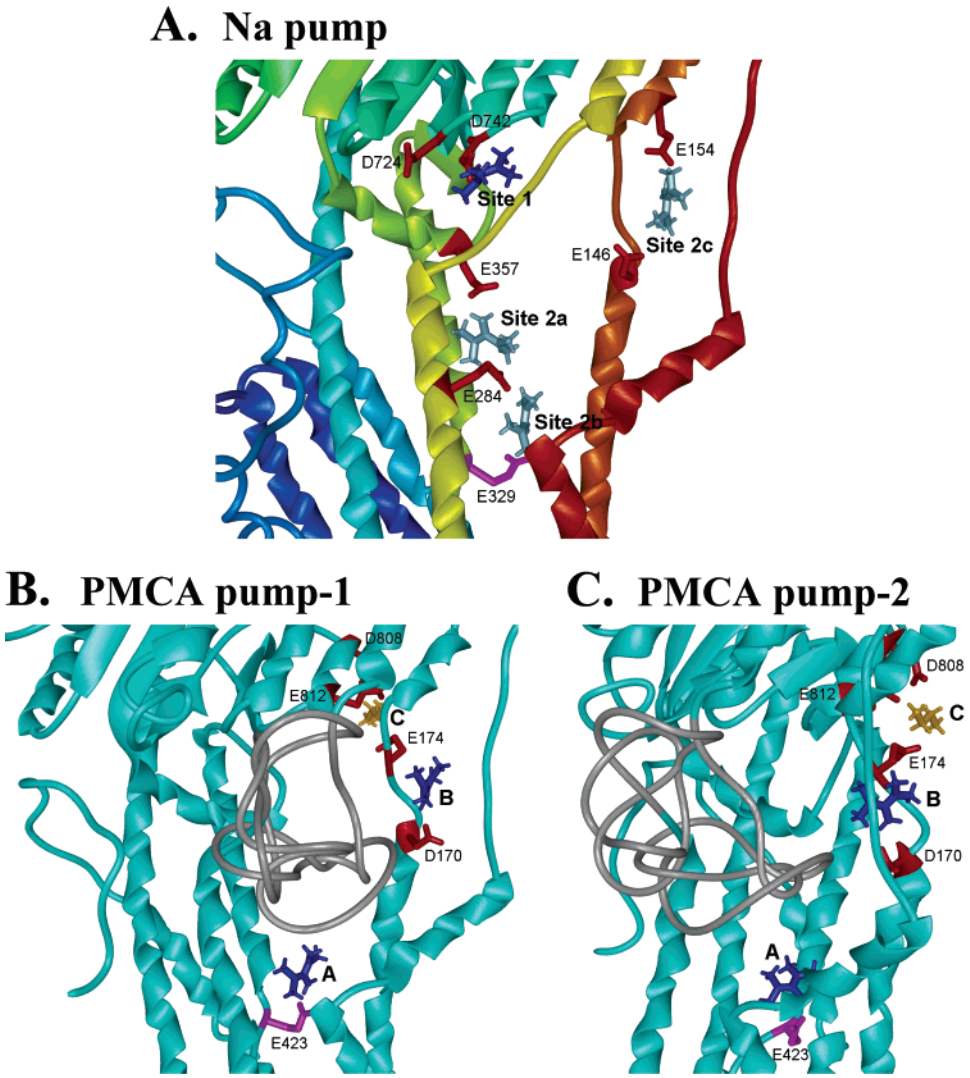

FIGURE 14: Comparison of TMG binding between Na pump and PMCA. (A) Possible sites for the second TMG binding site on Na pump. In this model, TMG was placed at the most favorable location (* in Figure 13) and then the docking procedure was repeated and there were three energetically favorable locations for the second TMG molecule (site 2a, b, and c). Acidic residues are red except E^{329} (in magenta). The side chains of the key residues (e.g., E^{146}, E^{154}, E^{329}, E^{284}, E^{357}, D^{742}) are displayed in stick mode. Site 1 (*) for TMG is dark blue; the three predictions for the possible location of site 2 for TMG are light-blue. (B and C) Two different views of PMCA. The red side chains are important conserved negatively charged residues. The magenta side chain is the access residue (e.g., E^{309}, SERCA; E^{329}, Na pump; E^{423}, PMCA). The blue (or light blue) ligand is TMG representing the possible binding sites of TMG (or GUA). In panel C, the gold molecule denotes ethyl diamine (site C). A large amino acid insertion in PMCA is in gray. Because of to the large loop, site 1 and 2a in Na pump were ignored in PMCA.

Divalent ethyl diamine inhibited the Na pump better than PMCA and appeared to be exclusively inside on the Na pump. Also, unlike Na pump inhibition, ethyl diamine did not appear to compete with Ca^{2+}, so presumably it does not impede binding to the transport site or access to the site.

What Conformations Do the Experiments and the Models Examine? Historically, the pump cycle has been described in terms of E1 and E2 conformations; however, over the years these terms have been defined differently by different investigators (see ref *45*). Many investigators use E1 to refer to pump conformations in which the transport site faces cytoplasmically and E2 to refer to those conformations with the transport site facing extracellularly. Some investigators use E1 to refer to Na^+ (or Ca^{2+}) bound conformations and E2 to refer to K^+ (or H^+) bound conformations. These are not necessarily self-consistent. For example, K^+ stimulates pNPPase activity and thus pNPPase might be called an E2 property, but the data clearly show that pNPPase is activated by cytosolic K^+ (*7*), and thus this is a cytosolic ion effect. To avoid this problem, we prefer to use the terms Ein and Eout (and Eoccluded) which refer to whether the transport sites face the cytoplasm (Ein), the extracellular media (Eout), or has access to neither (Eoccluded). In this formulation, extracellular ion effects would include K^+-activation of ATPase and K^+-stimulation of dephosphorylation, whereas intracellular ion effects include Na^+-activation of ATPase, K^+-activation of pNPPase and Na stimulation of phosphorylation. Almost all of the ions examined here show inside effects. Except for TPA inhibition of Na pump and ED inhibition of PMCA, all the ions primarily compete with Na^+ (or Ca^{2+}) for ATPase and with K^+ for pNPPase. Thus, one simple interpretation of the experiments is that organic cations bind to Ein, the pump without cations bound and with intracellular access. Unfortunately, this conformation has not been crystallized. However, the two adjacent conformations in the SERCA cycle have been crystallized,

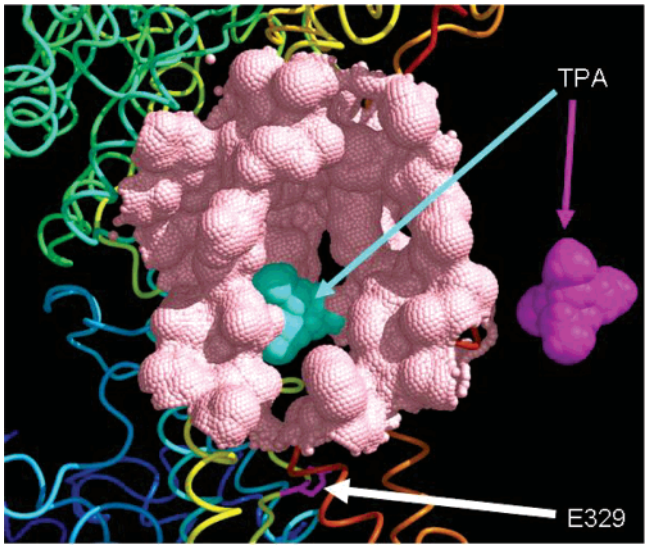

FIGURE 15: TPA is too large to access cytoplasmic binding site in Na pump. An illustration of how tight the Na pump entrance pathway is for TPA. The molecular surface near the entrance pathway is shown in pink. Residue, E^{329} (stick mode) is in magenta. TPA is shown in ball mode and colored in cyan embedded within the entrance to the access pathway. A separate TPA molecule is displayed on the right of the pump in magenta to show its full size. Note: TPA might still be able to go through the entrance after continuously, carefully adjusting its orientations without atomic clashes, but this is entropically unfavorable.

E(H) and E(Ca), although the former also required the presence of thapsigargin. Competition between the organic cations and Na^+ for ATPase or K^+ for pNPPase would seem to imply that the organic cations should not bind to either E(Na) or E(K), yet the homology model shows that there is a reasonable binding of the organic cations to the structure analogous to E(K). As discussed below, this is consistent with the possibility that E(K)TMG might exist and since K^+ and TMG are in competition, high K^+ should displace TMG thus allowing for the possibility that E(K)K exists. In contrast, the modeling did not identify any binding to 1SU4 presumably because the access area is "closed" in that structure, in part due to the extension of TM1.

Relation to Previous Work. While we have found no previous studies examining the effect of these organic cations on PMCA, there have been a number of studies on the Na pump.

Guanidines. Guanidines are often regarded as Na mimics as the guanidinium derivative, amiloride, inhibits Na channels and Na/H exchange as well as the Na pump. Our data suggest that, like Na ions, guanidine (and its derivatives) binds with higher affinity inside than outside. For example, competition with Na^+ (Figure 8A) but not K^+ (unpublished observations) for Na,K-ATPase activity is consistent with a cytoplasmic inhibition of guanidine. Likewise, competition with K^+ for pNPPase activity also points to binding to an inside facing site (Figure 8B); it has been shown that intracellular K^+ is sufficient for activation of pNPPase (*7*).

David et al. (*46*) have shown that the bis-guanidine compounds, *para*- and *meta*-xylylenebisguanidine (pXBG and mXBG), compete with both Na^+ and Rb^+ for occlusion within the enzyme. This inhibition of occlusion was suggested to be from the cytoplasmic surface as the binding of mXBG to the FITC-labeled enzyme produced an "E1" fluorescence signal similar to the binding of Na^+, and this signal was reversed by the addition of Rb^+ (*46*). An interesting observation by these investigators was that bis-guanidine compounds were more potent inhibitors than mono-guanidine compounds (*46*). These observations fit nicely with our current findings which suggest a cooperative effect on guanidine binding (Figure 7). David et al. (*46*) suggested that the apparent cooperative effect was due to an increased partitioning of the mono-guanidine compounds into the lipid at low ionic strength and thus effectively reducing the free inhibitor concentration compared to the bisguanidine compounds. The necessity for high enzyme concentrations and low ionic strength is a constraint of the Rb^+-occlusion experiments performed in the earlier study which is avoided in ATPase and pNPPase experiments. The fact that the Dixon plots are nonlinear indicates that more than one guanidine ion can bind. The best model to our data has each guanidine binding independently and inhibiting, but the binding of the first one greatly increases the affinity (by more than a factor of 10) for the second GUA molecule to bind. Consequently, our data strongly support a model in which the pump can bind at least two molecules of guanidine from the cytoplasmic side and thus suggest that the bis-guanidines could be more potent inhibitors because of the binding of both positive charges without any need to invoke different partition coefficients.

Quaternary Amines. Quaternary amines have been known to inhibit *K* channels and the Na,K-ATPase for more than three decades (*47*) and remain critical tools for deciphering structural and functional information about cation coordination (*48*). An extensive investigation of the extracellular effects of tetrapropylammonium (TPA) on the red cell Na pump was conducted by Kropp and Sachs (*49*). These authors concluded that TPA was a mixed-type inhibitor (with K^+_{ext}) of Na pump. In contrast, we recently presented data that strongly support a model in which extracellular TPA and K^+ compete for a common site (*40*). For example, in addition to K^+ and TPA competing for ATPase activity, we observed that TPA was able to decrease the rate of K^+-stimulated EP hydrolysis; K^+-stimulation of E_2P hydrolysis is known to occur via extracellular K^+ binding. An alternative explanation of the Kropp and Sachs (*49*) results is that TPA and K^+ compete at low TPA concentrations, similar to our results. They report binding constants of 1.8 and 3.6 mM for TPA binding to the pump in the absence of K^+ and with one K^+ bound, respectively. The TPA binding constant increases nearly 50-fold to 170 mM when two K^+ ions are bound (*49*); it seems likely that at very high TPA, there might be an additional site where TPA binds.

We also concluded that TPA could not bind to the cytoplasmic cation site as TPA did not compete with K^+ for pNPPase activity (*40*). Yet, our current data suggest that TEA does compete with K^+ for pNPPase activity, consistent with Sachs and Conrad (*47*) studies finding that TEA, but not TMA, inhibited the pump. Since cytoplasmic *K* activates pNPPase, this suggests that TEA binds from the cytoplasmic face. We were left with the puzzle as to why TPA is not able to inhibit from the cytoplasm. The modeling results suggest that TPA is too large: to get the large TPA molecule (Figure 15, magenta) to penetrate into the channel (Figure 15, cyan blue) several physical manipulations were required to avoid many unfavorable atomic collisions. Thus, these

modeling results provide a reasonable explanation for our kinetic data showing that TPA is unable to bind to the inside-facing cation site, whereas TEA can. The modeling also revealed that TMA is too small to make adequate contacts for stable coordination. It is interesting to note that choline (i.e., β-hydroxyethyl trimethylammonium) can reach fairly high concentrations in some cells and these pumps need to be able to bind their alkali metal substrates in the presence of choline. Thus, the low affinity of quaternary ammonium compounds for cytoplasmic sites on these pumps might have resulted via selection against choline binding.

Alkyl Diamine Inhibition. Schuurmans Stekhoven and colleagues (*50*−*52*) reported that ethyl diamine (ED) was quite effective at inhibiting phosphorylation of Na,K-ATPase (K_i < 0.1 mM). In addition, Forbush (*53*) showed that ED competitively blocked Rb^+-occlusion but was ineffective at slowing the rate of Rb^+-deocclusion. Although not concluded by these investigators, taken together these data suggest that ED preferentially binds to the cytoplasmic side of the Na,K-ATPase. If true, one would predict that ED and K^+ would *not* compete for Na,K-ATPase but would compete for pNPPase. In fact, this is exactly what was revealed by measuring the K^+-dependence of both catalyzes in the presence and in the absence of ED (Figure 10B,C). Calculating the K_i for ED inhibition of pNPPase (Figure 10C) gave a value of 0.11 mM, which is similar to the value reported for inhibition of Na pump phosphorylation (*51*). The substantially increased potency of these bifunctional amines is consistent with the cooperativity observed for guanidine inhibition (see above).

We did observe that different size diamines inhibited differently. However, part of the different potency of diamine inhibition may be due to differences in p*K* of the compounds themselves. The diamines have two separately titratable groups (i.e., H_2N-R-NH_2; R = Et, Pr, Bu). The p*K* values for the two amine groups on both PD and BD are such that both amines should be predominantly protonated and positively charged at physiological pH (i.e., pK_1 and pK_2 for PD are 8.7 and 10.3; for BD are 9.4 and 10.4; *54*). In contrast, the two amines in ED have p*K* values that differ and span the physiological range (i.e., $pK_1 = 7.1$ and $pK_2 = 9.9$; *54*). Thus, it is likely that ED and PD are differentially charged at pH 7.4, i.e., +1 and +2, respectively (Figures 9 and 10 were performed at pH 7.4). Given that cooperative binding was observed with the guanidine compounds, one would predict that the dual charged diamines would be more effective inhibitors. Indeed, this appeared to be the case for Na pump inhibition, where a 10-fold increase in $[H^+]$ substantially increased the inhibitory efficacy of ED; interestingly, the same pH change made PD a slightly weaker inhibitor (Figure 11A). Since the charge on PD should be +2 at 7.4 and cannot increase with higher $[H^+]$, we take this result to suggest a change in the protonated state of the Na pump amino acid residue that is part of the binding site that contacts PD (Figure 11A). For ED, a substantial fraction of the molecules are in the +1 state at pH 7.4 and lowering the pH to 6.4 increased the fraction in the +2 state; consequently, the increased efficacy of ED+2 must outweigh the reduced binding affinity accompanying the titration of the pump residue seen for PD. For PMCA, decreasing the pH from 7.4 to 6.8 had no effect on the inhibition by PD, suggesting that neither PD nor the organic cation binding site of the Ca pump were titrated over this pH range (Figure 11B). In contrast, the increased $[H^+]$ promoted the inhibition by ED (Figure 11B), consistent with the conclusion that the +2 charge of diamines is the more potent inhibitor of P-type ATPases.

Where Do these Ions Bind? TEA, GUA, TMG, and BD competed with cytoplasmic alkali ligands. ED also competed on the Na pump, although not on PMCA. Presumably, all the compounds that compete bind at the same site. We consider four possible models: (i) compete for binding at transport sites, (ii) compete for binding to access channel, (iii) bind to *K* modifier site, (iv) bind to access channel in E2 with occluded ion present.

(i) Transport Sites. Upon the basis of the SERCA structures, these compounds seem too large to get into a transport binding pocket. However, because SERCA (or Na pump or PMCA) have not been crystallized in a conformation with the transport sites empty we cannot rule out this possibility completely.

(ii) Compete for Binding to Access Channel. Kinetically, this is very plausible. Na^+ and K^+ or Ca^{2+} are thought to bind at the access on their way to the transport site and thus high enough concentrations of the transport substrates would displace the organic cations and prevent pump inhibition (*19*). On the other hand, at low Na^+, K^+ or Ca^{2+}, the organic cations would bind to the access channel and either screen the protein's negative charge density at this point, thus decreasing the probability of the transport substrates binding. Alternatively, if the substrate cations did bind, then presumably the inhibitory organic cation bound pump could not change conformation and occlude the alkali metal ions. The homology models show that it is reasonable to suggest that these molecules fit in that space—in fact, the homology models are also consistent with the experimental data that TPA does not fit for either pump and that TMA is too small. Thus, there is a remarkable consistency between the modeling and the experimental data despite the ambiguities associated within homology modeling and the fact that a structure of the kinetically correct conformation (i.e. inside open and empty) does not yet exist.

(iii) Bind to K Modifier Site. Both SERCA and PMCA activity increase in the presence of K^+ or Na^+. Recently, Sorensen and co-workers (*55*) have located this K^+ site on SERCA and shown that this region is homologous in the different pumps, including the Na pump. Some effects of cytoplasmic K^+ are consistent with a non-transport site effect of K^+ on the Na pump as well. However, kinetically, our results on PMCA are not easily reconciled with binding to the K^+ modifier site because Ca^{2+} displaces the organic cations, whereas Ca^{2+} is not thought to displace K^+ from the modifier site in SERCA.

(iv) Bind to Access Channel in E2 with Occluded Ion Present. Kinetically, we find that the organic cations compete with K^+ or Na^+ or Ca^{2+}. Plus the homology models show that there are reasonable binding sites in the conformation analogous to E(H)thapsigargin. So if this conformation (that is, E(K) or E(H)) binds the organic cations it must also, at high transport ion (Na^+, Ca^{2+}, or K^+) concentrations, bind the transported ion, so that the organic cations are displaced and competitive inhibition is observed. In this case, this would be an alternative explanation for K^+ acceleration of K^+ deocclusion on the Na pump (*56*).

Conclusions. Experimentally, we have demonstrated that guanidines block both the Na and Ca pump by binding from the cytoplasmic surface and that two guanidine molecules bind cooperatively to produce this inhibition. In addition, we have convincingly shown that although alkyl ammonium compounds inhibit the Na pump, they are completely innocuous toward PMCA. In addition, we found that although the Na pump cytoplasmic access site excludes TPA (*40*), the smaller ethyl derivative (TEA) can bind and inhibit from inside. Cooperativity of binding is also consistent with the observation that ethyl diamine inhibits both pumps better when in the +2 state than the singly charged form.

ACKNOWLEDGMENT

We thank Dr. Hao-Yang Liu (Univ. of Missouri-Columbia) for his help on homology modeling of the Na pump.

REFERENCES

1. Kaplan, J. H. (2002) Biochemistry of Na, K-ATPase, *Annu. Rev. Biochem. 71*, 511−535.
2. Lutsenko, S., and Kaplan, J. H. (1995) Organization of P-type ATPases: significance of structural diversity, *Biochemistry 34*, 15607−15613.
3. Albers, R.W., Koval, G. J., and Siegel. (1968) Studies on the interaction of ouabain and other cardio-active steroids with sodium-potassium-activated adenosine triphosphatase. *Mol. Pharmacol. 4*, 324−336.
4. Post, R. L., Hegyvary, C., and Kume, S. (1972). Activation by adenosine triphosphate in the phosphorylation kinetics of sodium and potassium ion transport adenosine triphosphatase, *J., Biol. Chem. 247*, 6530−6540.
5. Milanick, M. A. (1990) Proton fluxes associated with the Ca pump in human red blood cells, *Am. J. Physiol. 258*, C552−C562.
6. Salvador, J. M., Inesi, G., Rigaud, J. L., and Mata, A. M. (1998) Ca^{2+} transport by reconstituted synaptosomal ATPase is associated with H^+ countertransport and net charge displacement, *J Biol. Chem. 273*, 18230−18234.
7. Drapeau, P., and Blostein, R. (1980) Interactions of K^+ with (Na, K)-ATPase orientation of K^+- phosphatase sites studied with inside-out red cell membrane vesicles, *J. Biol. Chem. 255*, 7827−7834.
8. Raess, B. U., and Record, D. M. (1990) Inhibition of erythrocyte Ca^{2+}-pump by Ca^{2+} antagonists, *Biochem. Pharmacol. 40*, 2549−2555.
9. Missiaen, L., De, S. H., Droogmans, G., Wuytack, F., Raeymaekers, L., and Casteels, R. (1990) Ruthenium red and compound 48/80 inhibit the smooth-muscle plasma-membrane Ca^{2+} pump via interaction with associated polyphosphoinositides, *Biochim. Biophys. Acta* (1023), 449−454.
10. Toyoshima, C., Nomura, H., and Sugita, Y. (2003) Structural basis of ion pumping by Ca^{2+}-ATPase of sarcoplasmic reticulum, *FEBS Lett. 555*, 106−110.
11. Toyoshima, C., Nakasako, M., Nomura, H., and Ogawa, H. (2000) Crystal structure of the calcium pump of sarcoplasmic reticulum at 2.6 Å resolution, *Nature 405*, 647−655.
12. Toyoshima, C., and Nomura, H. (2002) Structural changes in the calcium pump accompanying the dissociation of calcium, *Nature 418*, 605−611.
13. Toyoshima, C., and Mizutani, T. (2004) Crystal structure of the calcium pump with a bound ATP analogue, *Nature 430*, 529−535.
14. Picard, M., Toyoshima, C., and Champeil, P. (2005) The average conformation at micromolar [Ca^{2+}] of Ca^{2+}-atpase with bound nucleotide differs from that adopted with the transition state analog ADP. AlFx or with AMPPCP under crystallization conditions at millimolar [Ca^{2+}], *J. Biol. Chem. 280*, 18745−18754.
15. Toyoshima, C., Nomura, H., and Tsuda, T. (2004) Lumenal gating mechanism revealed in calcium pump crystal structures with phosphate analogues. *Nature 432*, 361−368.
16. Sorensen, T L-M., Moller, J. V., Nissen, P. (2004) Phosphoryl transfer and calcium ion occlusion in the calcium pump, *Science 304*, 1672−1675.
17. Olesen, C., Sorensen, T L-M., Nielsen, R. C., Moller, J. V., Nissen, P. (2004) Dephosphorylation of the calcium pump coupled to counterion occlusion, *Science 306*, 2251−2255.
18. Lee, A. G., and East, J. M. (2001) What the structure of a calcium pump tells us about its mechanism, *Biochem. J. 356*, 665−683.
19. Schneeberger, A., and Apell, H. J. (2001) Ion selectivity of the cytoplasmic binding sites of the Na, K-ATPase: II. Competition of various cations, *J Membr. Biol. 179*, 263−273.
20. Milanick, M. A., Arnett, A. L., Helms, J. B., Prasse, M., and Gatto, C. (2004) Differential size exclusion between the inside and outside facing cation sites of the Na, K-ATPase, *Biophys. J. 86*, 495a.
21. Gatto, C., Helms, J. B., Huang, S.-Y., Zou, X., Arnett, K. L., and Milanick, M. A. (2005) Testing the accuracy of homology modeling: similar inhibition patterns by cytosolically acting organic cations on Na, K- and PM Ca-ATPase, *J. Gen Physiol. 126*, 17a.
22. Jorgensen, P. L. (1974) Purification and characterization of (Na^+ plus $K^{+)}$-ATPase. IV. Estimation of the purity and of the molecular weight and polypeptide content per enzyme unit in preparations from the outer medulla of rabbit kidney, *Biochim. Biophys. Acta 356*, 53−67.
23. Lowry, O. H., Rosebrough, N. J., Farr, A. L., and Randall, R. J. (1951) Protein measurement with the folin phenol reagent, *J. Biol. Chem. 193*, 265−275.
24. Gatto, C., and Milanick, M. A. (1993) Inhibition of the red blood cell calcium pump by eosin and other fluorescein analogues, *Am. J. Physiol. 264*, C1577−C1586.
25. Costa, C. J., Gatto, C., and Kaplan, J. H. (2003) Interactions between Na, K-ATPase alpha-subunit ATP-binding domains, *J. Biol. Chem. 278*, 9176−9184.
26. Jorgensen, P. L., and Farley, R. A. (1988) Proteolytic cleavage as a tool for studying structure and conformation of pure membrane-bound Na^+, K^+-ATPase, *Methods Enzymol. 156*, 291−301.
27. Berman, H. M., Westbrook, J., Feng, Z., Gilliland, G., Bhat, T. N., Weissig, H., Shindyalov, I. N., and Bourne, P. E. (2000) The Protein Data Bank, *Nucleic Acids Res. 28*, 235−242.
28. Sweadner, K. J., and Donnet, C. (2001) Structural similarities of Na, K-ATPase and SERCA, the Ca^{2+}-ATPase of the sarcoplasmic reticulum, *Biochem. J. 356*, 685−704.
29. Altschul, S. F., Madden, T. L., Schaffer, A. A., Zhang, J., Zhang, Z., Miller, W., and Lipman, D. J. (1997) Gapped BLAST and PSI-BLAST: a new generation of protein database search programs, *Nucleic Acids Res. 25*, 3389−3402.
30. Zhou, H., and Zhou, Y. (2005) SPEM: improving multiple sequence alignment with sequence profiles and predicted secondary structures, *Bioinformatics 21*, 3615−3621.
31. Green, N. M. (1989) ATP-driven cation pumps: alignment of sequences, *Biochem. Soc. Trans. 17*, 972.
32. Marti-Renom, M. A., Stuart, A. C., Fiser, A., Sanchez, R., Melo, F., and Sali, A. (2000) Comparative protein structure modeling of genes and genomes, *Annu. Rev. Biophys. Biomol. Struct. 29*, 291−325.
33. Case, D. A., Pearlman, D. A., Caldwell, J. W., Cheatham, I. I. I., T. E., Wang, J., Ross, W. S., Simmerling, C. L., Darden, T. A., Merz, K. M., Stanton, R. V., Cheng, A. L., Vincent, J. J., Crowley, M., Tsui, V., Gohlke, H., Radmer, R. J., Dauan, Y., Pitera, J., Massova, I., Seibel, G. L., Singh, U. C., Weiner, P. K., and Kollman, P. A. (2002) AMBER 7, San Francisco, CA, University of California.
34. Bruno, I. J., Cole, J. C., Edgington, P. R., Kessler, M., Macrae, C. F., McCabe, P., Pearson, J., and Taylor, R. (2002) New software for searching the Cambridge Structural Database and visualizing crystal structures, *Acta Crystallogr. B 58*, 389−397.
35. Ferrin, T. E., Huang, C. C., Jarvis, L. E., and Langridge, R. (1988) The MIDAS display system., *J. Mol. Graphics 6*, 13−27.
36. Ewing, T. J. A., and Kuntz, I. D. (1997) Critical evaluation of search algorithms for automated molecular docking and database screening., *J. Comput. Chem. 18*, 1175−1189.
37. Liu, H.-Y., Kuntz, I. D., and Zou, X. (2004) Pairwise GB/SA scoring function for structure-based drug design 12, *J. Phys. Chem. 108*, 5453−5462.
38. Zou, X., Sun, Y., and Kuntz, I. D. (1999) Inclusion of solvation in ligand binding free energy calculations using generalized Born model. *13*, *J. Am. Chem. Soc. 121*, 8033−8043.
39. Moller, J. V., Juul, B., and le Maire, M. (1996) Structural organization, ion transport, and energy transduction of P-type ATPases, *Biochim. Biophys. Acta 1286*, 1−51.

40. Gatto, C., Helms, J. B., Prasse, M. C., Arnett, K. L., and Milanick, M. A. (2005) Kinetic characterization of tetrapropylammonium inhibition reveals how ATP and Pi alter access to the Na^+-K^+-ATPase transport site, *Am. J. Physiol. Cell Physiol. 289*, C302−C311.
41. Milanick, M. A., and Arnett, K. L. (2002) Extracellular Protons Regulate the Extracellular Cation Selectivity of the Sodium Pump, *J. Gen. Physiol. 120*, 497−508.
42. Lushington, G. H., Zaidi, A., and Michaelis, M. L. (2005) Theoretically predicted structures of plasma membrane Ca^{2+}-ATPase and their susceptibilities to oxidation, *J. Mol. Graph. Model. 24*, 175−185.
43. Pinto, F. T., and Adamo, H. P. (2002) Deletions in the acidic lipid-binding region of the plasma membrane Ca^{2+} pump. A mutant with high affinity for Ca^{2+} resembling the acidic lipid-activated enzyme, *J. Biol. Chem. 277*, 12784−12789.
44. Obara, K., Miyashita, N., Xu, C., Toyoshima, I., Sugita, Y., Inesi, G., and Toyoshima, C. (2005) Structural role of countertransport revealed in Ca^{2+} pump crystal structure in the absence of Ca^{2+}, *Proc. Natl. Acad. Sci. 102*, 14489−14496.
45. Robinson, J. D., and Pratap, P. R. (1993) Indicators of conformational changes in the Na^+/K^+- ATPase and their interpretation, *Biochim. Biophys. Acta 1154*, 83−104.
46. David, P., Mayan, H., Cohen, H., Tal, D. M., and Karlish, S. J. (1992) Guanidinium derivatives act as high affinity antagonists of Na+ ions in occlusion sites of Na^+, K^+- ATPase, *J. Biol. Chem. 267*, 1141−1149.
47. Sachs, J. R., and Conrad, M. E. (1968) Effect of tetraethylammonium on the active cation transport system of the red blood cell, *Am. J. Physiol 215*, 795−798.
48. Peluffo, R. D., Hara, Y., and Berlin, J. R. (2004) Quaternary organic amines inhibit Na, K pump current in a voltage-dependent manner: direct evidence of an extracellular access channel in the Na, K-ATPase, *J. Gen. Physiol. 123*, 249−263.
49. Kropp, D. L., and Sachs, J. R. (1977) Kinetics of the inhibition of the Na-K pump by tetrapropylammonium chloride, *J. Physiol. 264*, 471−487.
50. Schuurmans Stekhoven, F. M., Swarts, H. G., Lam, G. K., Zou, Y. S., and De Pont, J. J. (1988) Phosphorylation of (Na^+ + K^+)-ATPase; stimulation and inhibition by substituted and unsubstituted amines, *Biochim. Biophys. Acta 937*, 161−76.
51. Van der Hijden, H. T., Schuurmans S. tekhoven, F. M., and De Pont, J.J. (1989) Sidedness of the effect of amines on the steady-state phosphorylation level of reconstituted $Na^{+/}K^+$-ATPase, *Biochim. Biophys. Acta 987*, 75−82.
52. Schuurmans Stekhoven, F. M., Zou, Y. S., Swarts, H. G., Leunissen, J., and De Pont, J.J. (1989) Ethylenediamine as active site probe for Na^+/K^+-ATPase, *Biochim. Biophys. Acta 982*, 103−114.
53. Forbush, B., III (1988) The interaction of amines with the occluded state of the Na, K-pump, *J. Biol. Chem. 263*, 7979−7988.
54. Ohtaki, H., and Tanaka, N. (1971) Ionic equilibria in mixed solvents. VI. Dissociation constants of aliphatic diamines in water-methanol solutions, *J. Phys. Chem. 75*, 90−92.
55. Sorensen, T. L., Clausen, J. D., Jensen, A. M., Vilsen, B., Moller, J. V., Andersen, J. P., and Nissen, P. (2004) Localization of a K^+-binding site involved in dephosphorylation of the sarcoplasmic reticulum Ca^{2+} -ATPase, *J. Biol. Chem. 279*, 46355−46358.
56. Forbush, B. (1987) Rapid release of ^{42}K and ^{86}Rb from an occluded state of the Na, K-pump in the presence of ATP or ADP, *J. Biol. Chem. 262*, 11104−11115.

BI060667J